

Investigation of Leading Edge Film Cooling Jets In A Cross Flow

Dr A. H. Yousif
Professor
University of Technology

Dr K. J. M. Al-Khishali
Assist. Professor
University of Technology

Dr Muna S Kassim
Lecture
Al Mustansiriya University

Abstract

The thermal effect of the turbine blade film cooling and the penetration area of jets issuing at an angle into cross mainstream flow have been investigated numerically and experimentally. Experimental and numerical simulations have been introduced to simulate a discrete circle hole film cooling flow over a symmetrical airfoil representing turbine guide vanes surface. Several cases have been studied in the experimental work by using three-velocity ratio (0.5, 0.9, 1.3), and three different jet issuing angles, longitudinal injection angle (37.5^0 and 90^0) both with lateral injection angle (stagger angle = 0^0 and 45^0). Airfoil angle of attack has been changed during the experimental program throughout (0^0 , 5^0 , 10^0 , and 15^0). Experimental investigations gave qualitative information about the penetration area and flow structure of the mixing flow at all cases and the results were used to verify the computation method and to select the best velocity ratios for the flow penetration, flow structure, and the thermal effect of cool jets. An accepted agreement between the experimental and computational results found from model (a) ($\beta=37.5^0$ and $\theta=0^0$) for velocity ratio ($VR=0.5$) and blade angle of attack ($\alpha=0^0$). Computational results show hole rows spacing and issuing angle for maximum film cooling effectiveness (cooling efficiency)

Key words: turbine blade, film cooling, penetration area, jet angle, mixing flow

الخلاصة

يتناول هذا البحث إجراء اختبار عددي وتجريبي للتأثير الحراري لغشاء التبريد لريشة التوربين الغازي ومنطقة الانتشار بين نفاثات هواء التبريد الذي يضخ بزاوية مع جريان الهواء الرئيسي. لقد تم محاكاة أفتحة الدائرية لنفاثات التبريد عددياً وتجريبياً على مقطع ريشه تمثل سطح زعانف التوجيه للتوربين. لقد تم تجريبياً إجراء اختبارات لثلاث نسب جريان هي 0.5, 0.9, 1.3 وزاويتي نفث على امتداد الجريان هي 37.5^0 و 90^0 درجة وزاويتي نفث عرضيتين هي 0^0 و 45^0 درجة وأربعة زوايا هجوم لمقطع الريشه هي 0^0 و 5^0 و 10^0 و 15^0 درجة. لقد أعطت التجارب معلومات قيمه لمنطقة الانتشار وهيكل جريان الخليط لكل الحالات وقد وجد توافق جيد ومقبول بين النتائج التجريبية ونتائج الحل العددي للنموذج (a) ($\beta=37.5^0$ and $\theta=0^0$) لنسبة السرعة 0.5 وزاوية الهجوم صفر. نتائج الحل العددي بينت كذلك الفضائات المناسبة بين صفوف الفتحات وزاوية خروج النفاثات من الفتحات التي تعطي أفضل تأثير لغشاء التبريد، اي أفضل كفاءة تبريد.

Nomenclature

CFD	Computational Fluid Dynamic
c	Chord length (cm)
d	Hole diameter (cm)
K	Turbulent kinetic energy (m^2/sec^2)
	Diffusion in j-direction
i and j	suffixes represent the co-ordinate direction
NACA	National Advisory Committee of Aeronautics
T	Time-averaged temperature (0K)
T_J, T_{in}	Jet temperature and inlet temperature respectively (0K)
TET	Turbine entry temperature (0K)
t	Time (sec)
S_{bj}	Buoyancy source or sink term
S_ϕ	Source or sink
VR	Velocity ratio
u, v and w	Velocity component in x, y and z direction respectively
x, y and z	Physical or Cartesian Coordinates
y^+	Dimensionless distance
ϕ	Scalar property
α	Blade angle of attack ($^\circ$)
β	Jet angle with the horizontal axis ($^\circ$)
ε	Rate of dissipation of (m^2/sec^3)
θ	Lateral injection angle ($^\circ$)
ρ	Air density (kg/
δ	Distance from the wall to the cell center (m)
μ	Dynamic Viscosity (m/N)
τ_w	Wall shear stress N/

1- Introduction

The blades/vanes in gas turbines require proper cooling mechanism to protect the airfoils from thermal stresses generated by exposure to hot combustion gases. The problem becomes aggravated by the growing trend of using higher turbine inlet temperature to generate more power. Thus, film cooling is used as a cooling mechanism and it works in the form of a row of holes in the span wise directions of the blade, from which a cold jet is issued into the hot cross flow. The mixing process during the penetration of the cold jet into the hot gas creates a three-dimensional flow field. The resulting temperature downstream of the jet, the trajectory and physical path of the jet are critical design parameters ^[1]. Film cooling flows are characterized by cooling jet injected at an angle from the blade surface into the heated cross flow.

The resulting flow field is quite complex, and accurate predictions of the flow and heat transfer are difficult to obtain, particularly in the near field of the injected jet ^[2]. Therefore the flow penetration, flow structure, and the thermal effect of cool jets issuing into an incompressible hot cross flow at an angle over an airfoil which represents the turbine blade surface are the main subject in the present study. In order to provide an assessment of the performance of different models, a film cooling configuration that was geometrically simple, but which incorporated all the essential physics of the film cooling problem was chosen.

2- Experimental set-up

A useful and quick procedure for obtaining qualitative information on the effectiveness and flow behaviors of different jet angles configurations is to make the flow of cooling air visible. The method used here utilizes smoke mixed with the cooling air to make it visible. This method is used to study cooling films build up on the turbine blades. The visual observations gave a good feeling of the best jet angle and the best velocity ratio for the well covered blade surface parts by the cooling air. The apparatus used to perform the experimental work are the test duct (similar to the test duct used by [3], compressor, blower, speed control, digital volt meter, digital ammeter, digital camera, and smoke generation system).

The experiments were performed in an open circuit low speed wind tunnel with rectangular duct. The airfoil was mounted horizontally across the test section. The walls of test duct are made of Plexiglas for visualization purposes. The inlet of the duct contains a fine meshed removable flow-smoothing screen acting as a filter to prevent unwanted particles from flowing in the air duct into test section. The test rig was designed and constructed by [4]. Three (a, b and c) geometrically (NACA 0021) airfoil models are employed in this study with different compound angle injection from one and two staggered rows arrangement. The holes, dimensions, arrangement and the injection angles used for the experimental study and flow visualization are;

1-Model (a): The number of holes is (9) on each side, the diameter of hole is $d= 1\text{mm}$. Distance between one hole and the other is $5d$, angle of injection $\beta= 37.5^\circ$ and the lateral injection angle [staggered, $\theta = 0^\circ$].

2-Model (b): Nine holes on each side, the diameter of each hole is $d= 1\text{ mm}$. Distance between one hole and the other is $5d$, angle of injection $\beta= 37.5^\circ$ and the lateral injection angle [staggered, $\theta = 45^\circ$].

3-Model (c): The number of the holes is (4) two on the upper side and the other on the lower side, the diameter of hole is $d= 2\text{ mm}$. Distance between one hole and the other is $17d$, angle of injection is $\beta= 90^\circ$ and the lateral injection angle [staggered, $\theta = 0^\circ$]. The schematic diagrams of (NACA 0021) airfoil models and holes arrangement are shown in Figure (1).

3- Penetration area

Figures (3 to 5) show the smoke injection jet and free stream flow photos for all cases. These photos gave the front view photos in x-y plane and show the general trend of the jet in cross flow. Greater area of jet penetration and jet-mainstream mixing are observed for angle of attack= 0 and $VR=0.5$, while close to the airfoil surfaces the jet penetration in cross flow seems to be not well, in which the area close to the surfaces were much less smoke. In the region of smoke domination the smoke brightness and darkness can be distinguished easily and disappeared gradually downstream as the mixing process continues. These photos also show that the separation bubble is formed in the penetration as (VR) increased and the number of bubbles increased as VR increased at both airfoil surfaces and seems to be larger at the upper surfaces than the lower ones.

Figure (4) shows a remarkable reduction in the penetration height case (b), in which the penetration height becomes approximately half that of case (a). For all cases the vortices are formed and the separation point progresses form close to the trailing edge. Also for the three cases investigated the smoke construction in the jet core were dominated and the smoke vanished toward the penetration boarder, i.e., smoke constructed domination (smoke construction variation).From all experimental investigation the effect of penetration area closed to the blade surfaces will affect the rate of heat transfer due to boundary layer behavior at that point, that will lead to increase the coefficient of heat transfer hence improve blade protection from overheating.

4- Mathematical model

In order to develop an applicable comprehensive computational method, some reasonable assumptions have to be made, they are:-

The entering fluid flow is subsonic everywhere.

The fluid flow is incompressible.

The fluid flow is steady state.

The fluid flow is viscous.

The turbulence is isotropic.

The flow within the coolant hole is three-dimensional, as can be seen in the computational predictions of [2]. A separation at the hole inlet is the cause of a pair of counter-rotating vortices and a region of increased velocity opposite of the separation bubble. The blockage created by the jet as it enters the mainstream creates a local variation in pressure at the hole exit. After leaving the hole, the coolant mixes with the mainstream. An approximation of the entropy generated during this mixing process can be obtained by assuming the mixing takes place within a short distance downstream of the hole, thus justifying a constant static pressure by using the hole exit velocity and temperature. This mixing calculation is similar in character to the one-dimensional analytical model proposed by [5].

The increases in mass within a control volume must be equal to the mass out flow minus the mass in flow through the control volumes surface. The rate of change of energy is equal to the sum of the rate of heat addition to and rate of work done on a fluid particle (first law of thermodynamic). According to the above assumptions the mass within the control volume may be expressed mathematically for three dimensional incompressible fluids as:

$$\frac{du}{dx} + \frac{dv}{dy} + \frac{dw}{dz} \quad \dots (1)$$

The other fundamental equation that governs the flow of a fluid are derived from Newton's second law (the conservation of momentum). The equation is called the Navies-Stokes equation, and for incompressible flow may be expressed in compact cartesian tensor notation as given in [6] as:

$$\frac{\partial(\rho u_i)}{\partial t} + \frac{\partial(\rho u_j u_i)}{\partial x_j} = -\frac{\partial p}{\partial x_i} + \frac{\partial}{\partial x_i} \left[\left(\frac{\partial u_i}{\partial x_j} + \frac{\partial u_j}{\partial x_i} \right) \right] + S_{bj} \quad \dots(2)$$

Where the suffixes i and j represent the co-ordinate directions and (S_{bj}) are buoyancy source or sink terms. This leads to the governing equations of fluid flow to solve the mixing process of blowing air with cross flow in which this will generate complex flow. The blowing air after leaving the injection hole mixes with main stream. An approximation of the entropy generated during the mixing process can be obtained by assuming that the mixing process takes place within the short distance downstream of the hole, thus justifying a constant static pressure mixing calculation.

The mixing region is divided into several mixing control volumes in the vicinity of the blowing holes. In the mixing calculation the equations for the conservation of mass and momentum are applied to the mixing control volume. The blockage created by the blowing air enter the main stream creates a very small local variation of the pressure at the hole exit.

Thus, the static pressure is taken to be constant during the mixing process, using holes exit velocity. The outflow values of stagnation pressure from each of the mixing control volumes are mass averaged to determine the overall stagnation. This may be done with using the mixture laws given by [5].

Flow and heat transfer equations were solved by using the program structure method, which creates the geometry and grid. This method is used in the solver explicitly or implicitly. T-Grid is used to generate a tetrahedron and hexahedron, which are existing boundary mesh. This method is used in the solver explicitly or implicitly.

5- The (K-E) Turbulence Model

The eddy viscosity at each grid point is related to values of the turbulence kinetic energy (k) and the dissipation rate of turbulence energy (ϵ). The program creates standard form of the (k- ϵ (epsilon)) turbulent model is only valid in the fully turbulent regions of a flow. Consequently, in the code a different treatment will be made near solid walls, where viscous diffusion dominates turbulent diffusion according to [7].

In the current study the modified (k- ϵ) turbulence model [7] was adapted when the turbulent model was employed. The enhancement wall treatment potation has been selected to deal with the resolution of the boundary layer in present model. They introduced a mesh-dependent dimensionless distance ($y^+ = \delta \quad (\mu)$), that quantifies to what degree of wall layer resolved .After doing the calculations the value of (y^+) is observed for each mesh. The values of (y^+) are dependent on the resolution of the grid and flow Reynolds number, and are meaningful only in boundary layers. The value of y^+ in the wall-adjacent cells dictates how wall shear stress is calculated.

6- Choosing The Appropriate Grid Type

Grids mesh has kinds such as hexahedron, T-Grid to generate a tetrahedron, which are existing boundary mesh. Program code can use grids comprising of tetrahedron or hexahedron cells, or a combination of the two, in three dimensions. The choice for the problems involved complex geometries; the creation of structured or block-structured grids (consisting of hexahedron cells) can be extremely time-consuming, if not impossible. Set up time is, therefore, the major motivation for using unstructured grids employing tetrahedron cells, the range of length scales of the flow is large, and a tetrahedron mesh can often be created with far fewer cells than the equivalent mesh consisting of hexahedron cells.

This is because a tetrahedron mesh allows cells to be clustered in selected regions of the flow domain, whereas structured hexahedron meshes will generally force cells to be placed in regions where they are not needed, the reason behind this case in the current study of unstructured tetrahedron meshes were chosen as shown in Figure (1).

7- Boundary Conditions

To define a problem that results a unique solution must be specified. GAMBIT code defining boundary conditions involves information on the dependent (flow) variables at the domain boundaries. Boundary conditions specify the flow and properties variables on the boundaries of the physical model. The boundary conditions in GAMBIT are classified the flow inlet and exit boundaries: free stream temperature, free stream pressure, jet temperature, model wall surface and the internal face boundary conditions are defined on cell faces, which means that they do not have a finite thickness and they provide a means of introducing a step change in flow properties ^[8]. The far field boundary conditions are more difficult to specify in a way that facilitates computation. It is also necessary to differentiate between inflow and outflow boundary conditions, which can determine pressure far field, pressure outlet boundary condition.

The pressure outlet boundary conditions are used to define the static pressure at flow outlet. The use of a pressure outlet boundary condition instead of an outflow condition often results in a better rate of convergence when backflow occurs during iteration. Temperature boundary conditions are used to model a free stream incompressible flow at infinity, with free stream velocity and static conditions specified. The boundary conditions in finite volume techniques ^[9] are used to describe the flow in entry and exit of the solution domain which helps to select the most appropriate boundary condition in application. It provides pressure inlet, jet temperature and velocity, free stream temperature and velocity and wall surface of model ^[10].

8- Convergence

At convergence, all discrete conservation equations (momentum, energy, etc.) obey in all cells to a specify tolerance. Solution no longer changes with more iteration, solution to equation on overall mass, momentum, energy, and scalar balances are obtained. Monitoring convergence with residuals, generally shows, a decrease in residuals by three orders of magnitude indicating at least qualitative convergence, major flow features established and scaled species. Residual may need to decrease to 10^{-4} to achieve species balance, monitoring quantitative convergence and monitoring other variables for changes. This run aimed to convergence and the output is shown in Figure (2).

9- Computational Results

Analysis of computational results is taken at different sections of span-wise direction for the three models. These results are at $x/s= 0.5$ for models (a), (b), and at $x/s=0.1$ for model (c). The jet temperature contours were used to simulate jet penetration shape, since the other properties such as velocity vector, pressure; turbulent kinetic energy and turbulent dissipation energy do not give accurate jet shape behaviour due to the presence of high vortices associated with jet flow penetration. ^[11]

Figures from (5) to (10) show the temperature contours at $x/s = 0.5$ (mid-plane of span for $(\beta = 37.5^\circ$ and $\theta = 0^\circ$ and 45°) and at $x/s = 0.1$ for $(\beta = 90^\circ$ and $\theta = 0^\circ$). In all cases take into the consideration the injection through which the cool air issued is at four airfoil angles of attack (0° , 5° , 10° and 15°). The cool jet temperature is $(T_j) = 300^\circ\text{K}$ is injected into hot free stream of $(T_{in}) = 600^\circ\text{K}$ and 1500°K for $VR = 0.5, 0.9$ and 1.3 .

The flow is assumed to be a fully developed turbulent flow. A jet lift-off behavior of the contour rotating vortices of the hot free stream under the cool jet can be seen in these Figures. In fact, the coolant jet core has actually been divided into two regions at all blowing ratios. In all these Figures, high jet penetration in the vertical direction and jet-main stream mixing is observed for $(\alpha = 0^\circ, 5^\circ, 10^\circ$ and $15^\circ)$, while the penetration area in the stream-wise direction in horizontal plane appears to be wake close to airfoil surface. Thus, the horizontal cooling effect in stream-wise direction close to the surface showed very poor effect for $(VR) = 1.3$ angles of attack (10° and 15°).

The main point raised from these results, for $T_{in} = 600^\circ\text{K}$ and 1500°K and $T_j = 300^\circ\text{K}$, at $x/s = 0.5$ for models (a) and (b) and at $x/s = 0.1$ for model (c), is that the optimum holes rows spacing and low issuing angle for maximum film cooling effectiveness (cooling efficiency) was detected. When comparing the experimental and the computational results the percentage error between them with regard to penetration height for three the models did not exceed 6%. Also it was found that the maximum vertical penetration height appears at cases $(\beta = 90^\circ$ and $\theta = 0^\circ)$ for $(VR) = 0.5$ and $\alpha = 0^\circ$ are (1.5) and (1.15) cm respectively.

Therefore the case of $VR = 0.9$, the two cases of jet angles $(\beta = 37.5^\circ$ and $\theta = 0^\circ)$ and $(\beta = 90^\circ$ and $\theta = 0^\circ)$ for angles of attack $(\alpha = 0^\circ$ and $5^\circ)$ gives the most useful results, best cooling effectiveness and high jet penetration. This may be leads to use for the purpose of turbine guide vane blade film cooling applications. The blade (airfoil) angle of attack has been varied until optimum film cooling effectiveness, optimum value of the horizontal cooling effect, is obtained. Computational results show jets rows spacing and issuing angles for maximum film cooling effectiveness (cooling efficiency) agree well with predicted results of [12].

The results presented in Figures (11 to 13) show the velocity vector interaction between cold jet and hot cross flow for all cases. These interactions indicated that the flow structure downstream the inject holes and show complex structures involves the horseshoe vortex, counter rotating vortex pair and wake vortices. These structures can be used to control the jets penetration area and to estimate the jet flow spreading rate. By comparing these two figures it is clear to observed that the vortices size and shape generated downstream jet hole in case $(\alpha = 0^\circ)$ is smaller in size and the shape of vortex varied of that of case $(\alpha = 15^\circ)$.

10- Conclusion Remarks

The main conclusions raised from the above analysis are that, in order to increase the horizontal cooling distance (penetration area in horizontal plane) near the blade surface and to decrease the vertical penetration distance to agreeable distance, there were two methods may be used to do these desired requirements either by varying the velocity ratio depending upon jet inclination angles nor by decreasing the jets angles. In the present work a compromise has been done between these two methods and leads to use the experimental observation as a measure rule to obtain the most useful cases.

The interaction between the neighboring jets of enhances the turbulence intensity and diffusion downstream of the jets in the mainstream flow. These conclusions may be taken into account when selecting the span-wise spacing between each two neighboring jets of holes in the applications of film cooling. An accepted agreement between the experimental and computational results found for model (a) ($\beta = 37.50$ and $\theta = 00$) for velocity ratio ($VR = 0.5$) and blade angle of attack ($\alpha = 00$). Computational results show hole rows spacing and issuing angle for maximum film cooling effectiveness (cooling efficiency).

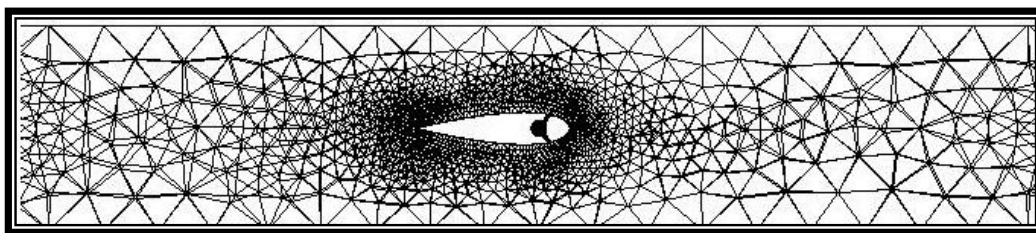


Figure (1) Tetrahedron Mesh

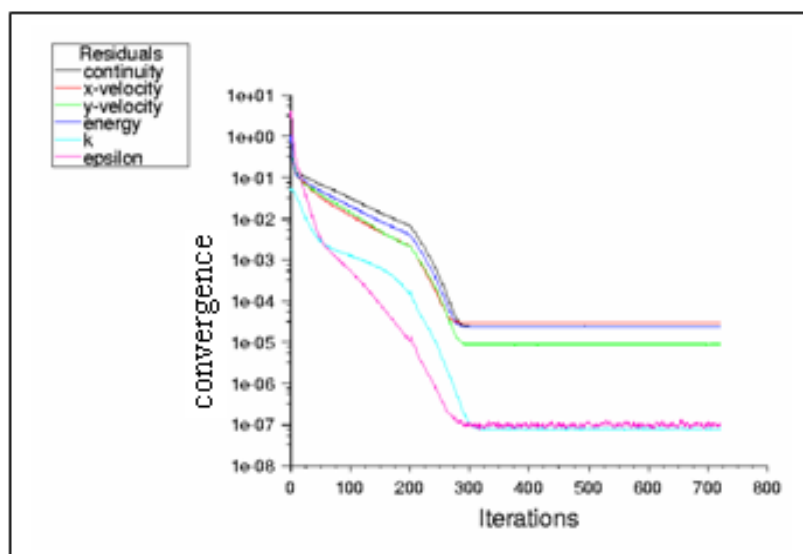
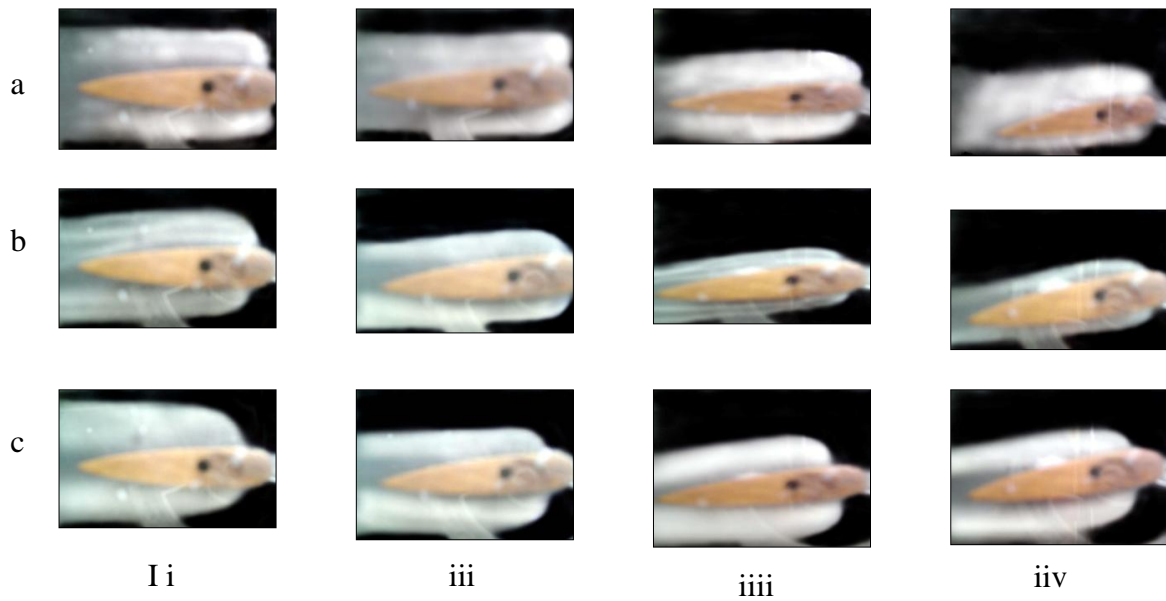
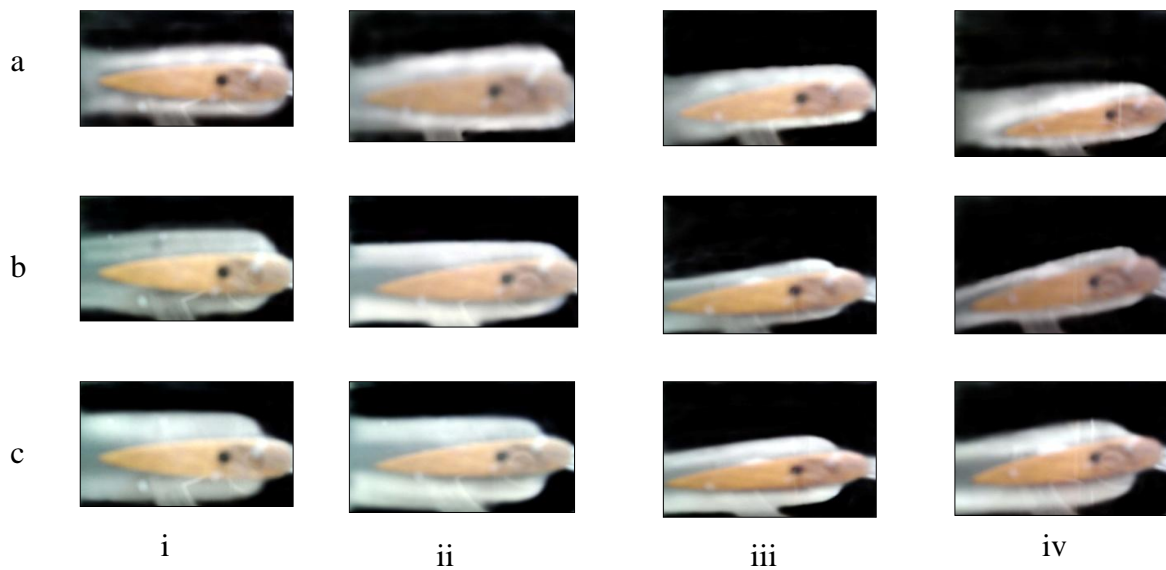


Figure (2) Convergence To Solve Discrete Conservation Equations



**Figure (3) Experimental Photos For Three Models With $VR=0.5$ And
i) $A= 0^\circ$, li) $A= 5^\circ$, lii) $A= 10^\circ$ And V) $A=15^\circ$.**



**Figure (4) Experimental photos for three models with $VR=0.9$ and
 $\alpha= 0^\circ$, ii) $\alpha= 5^\circ$, iii) $\alpha= 10^\circ$ and v) $\alpha=15^\circ$.**

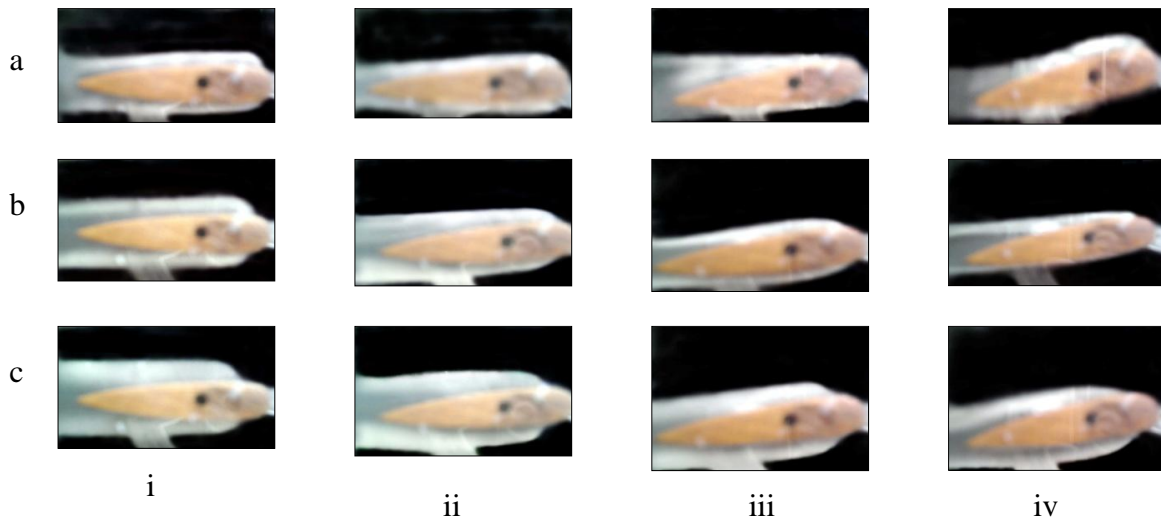


Figure (5) Experimental photos for three models with $VR=1.3$ and
 i) $\alpha=0^\circ$, ii) $\alpha=5^\circ$, iii) $\alpha=10^\circ$ and v) $\alpha=15^\circ$

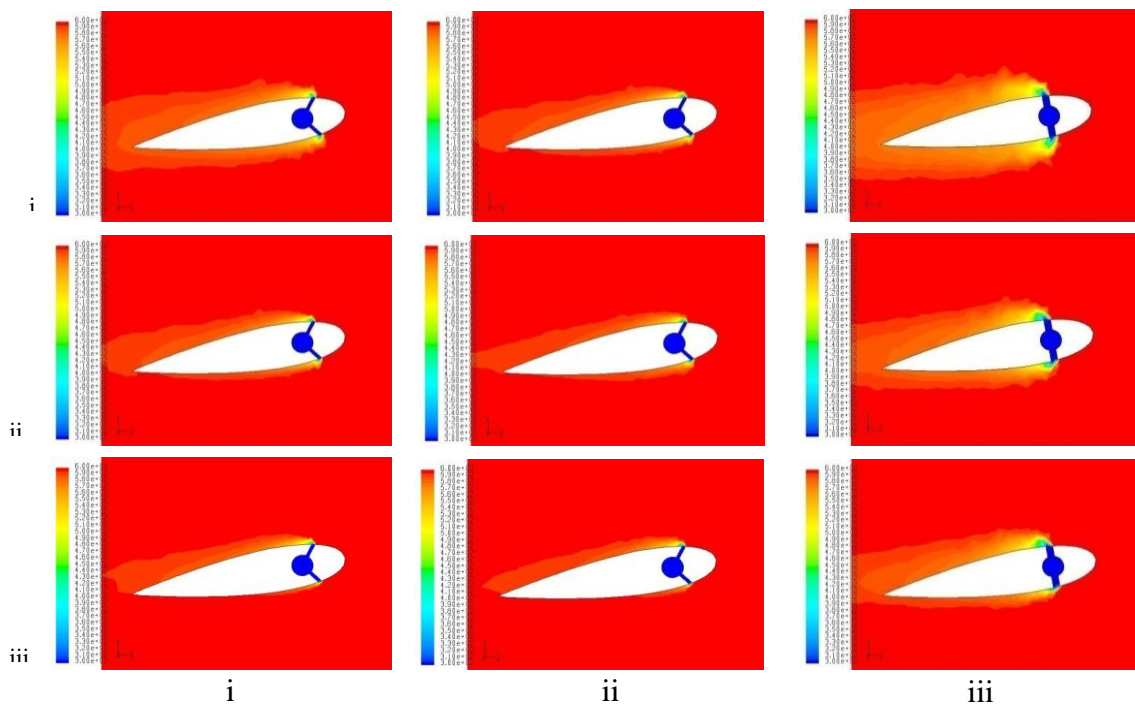


Figure (6) Temperature contours for $T_{in}=600\text{ K}$ and $T_f=300\text{ K}$ for three models
 with $\alpha=10^\circ$ and $VR=$ i) 0.5, ii) 0.9 and iii) 1.3.

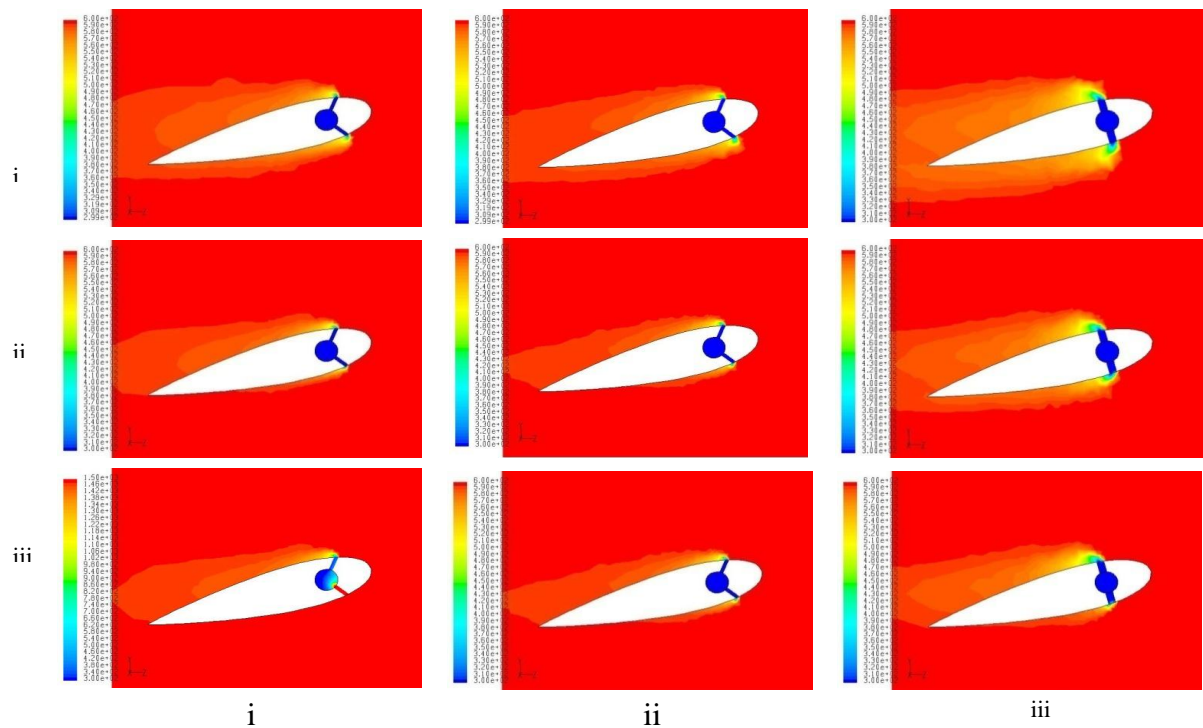


Figure (7) Temperature contours for $T_{in}= 600\text{ K}$ and $T_j=300\text{ K}$ for three models with $\alpha= 15^\circ$ and $VR=$ i) 0.5, ii) 0.9 and iii) 1.3.

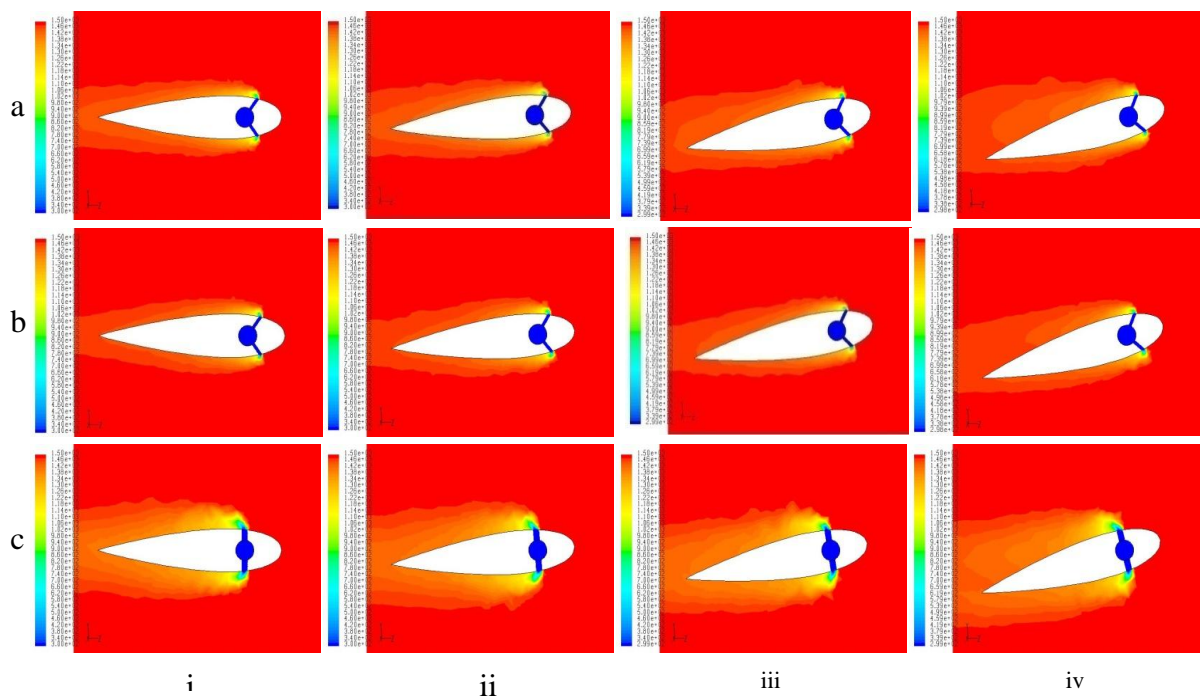


Figure (8) Temperature contours for $T_{in}=1500\text{K}$ and $T_j= 300\text{K}$ for three models with $VR=0.5$ and i) $\alpha= 0^\circ$, ii) $\alpha= 5^\circ$, iii) $\alpha= 10^\circ$ and v) $\alpha= 15^\circ$.

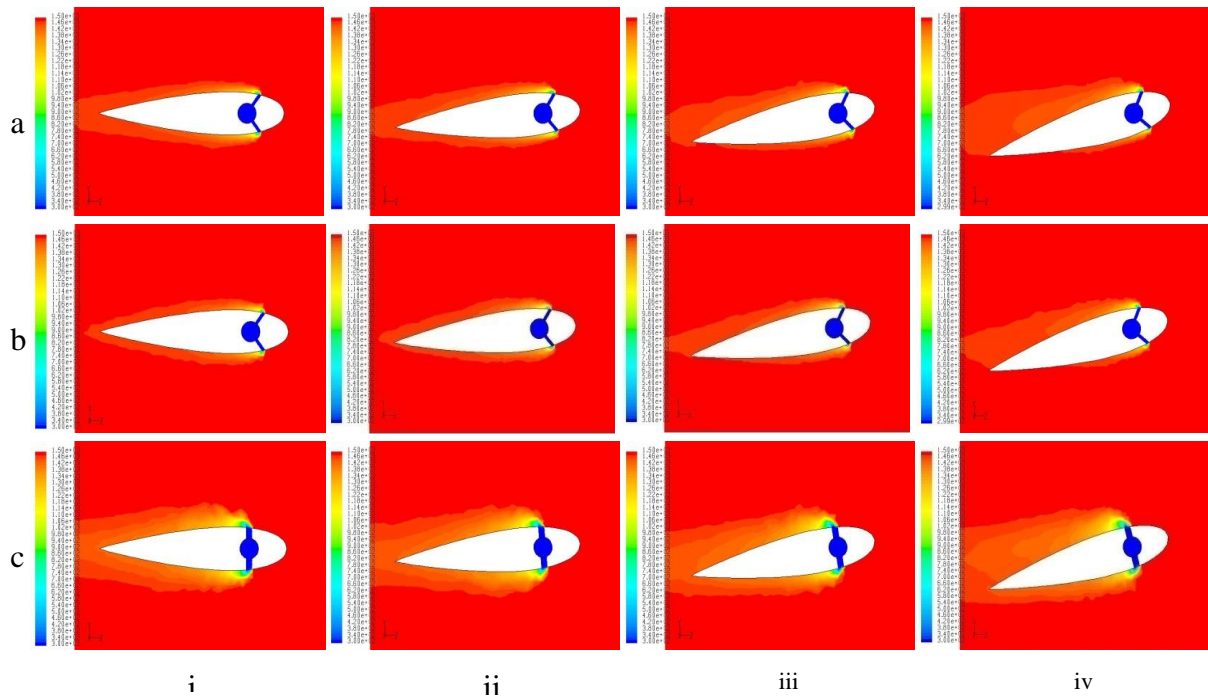


Figure (9) Temperature contours for $T_{in}=1500K$ and $T_j= 300K$ for three models with $VR=0.9$ and i) $\alpha= 0^\circ$, ii) $\alpha= 5^\circ$, iii) $\alpha= 10^\circ$ and v) $\alpha= 15^\circ$.

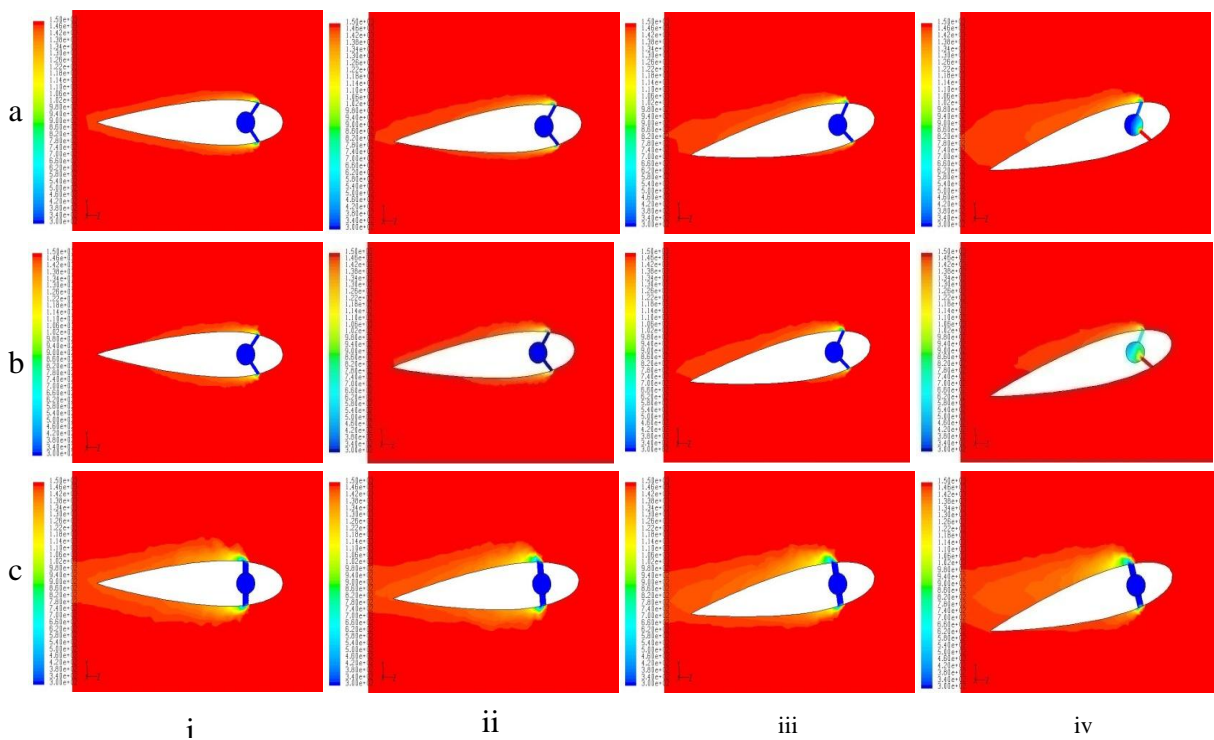


Figure (10) Temperature contours for $T_{in}=1500K$ and $T_j= 300K$ for three models with $VR=1.3$ and i) $\alpha= 0^\circ$, ii) $\alpha= 5^\circ$, iii) $\alpha= 10^\circ$ and v) $\alpha= 15^\circ$.

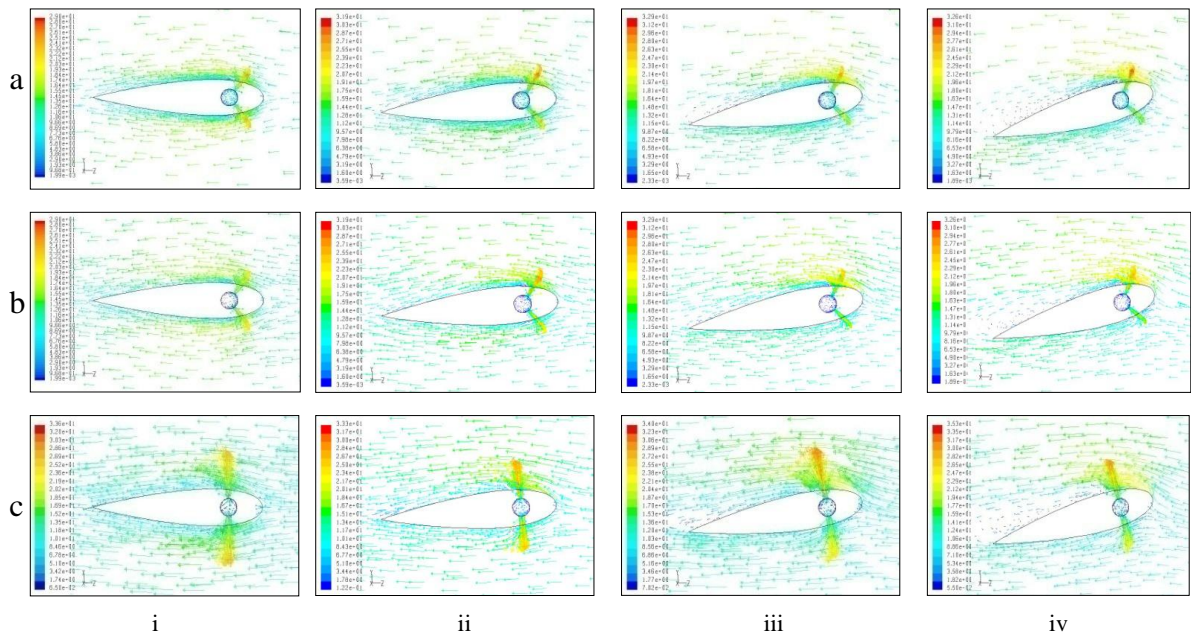


Figure (11) Velocity vectors at mid-plane of span for (a) and (b) and at $x/s=0.1$ from the injection point for (c) with $VR=0.5$ and i) $\alpha=0^\circ$, ii) $\alpha=5^\circ$, iii) $\alpha=10^\circ$ and v) $\alpha=15^\circ$.

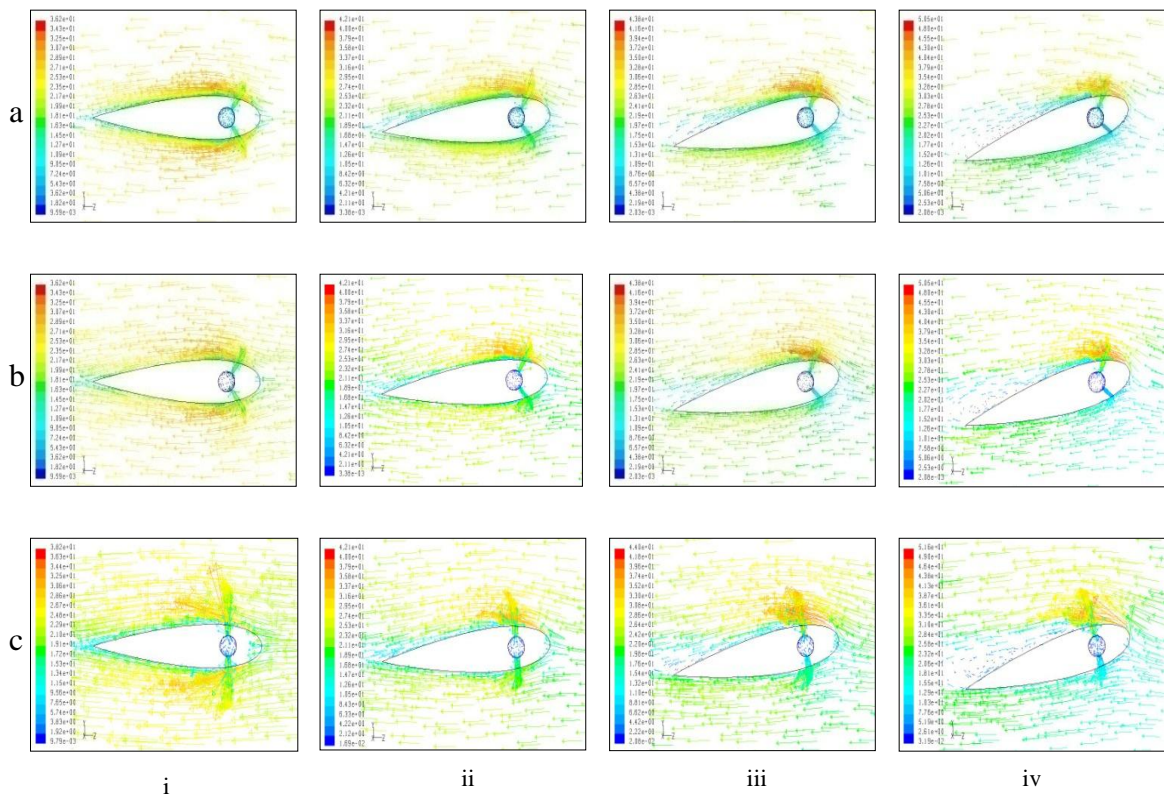


Figure (12) Velocity vectors at mid-plane of span for (a) and (b) and at $x/s=0.1$ from the injection point for (c) with $VR=0.9$ and i) $\alpha=0^\circ$, ii) $\alpha=5^\circ$, iii) $\alpha=10^\circ$ and v) $\alpha=15^\circ$.

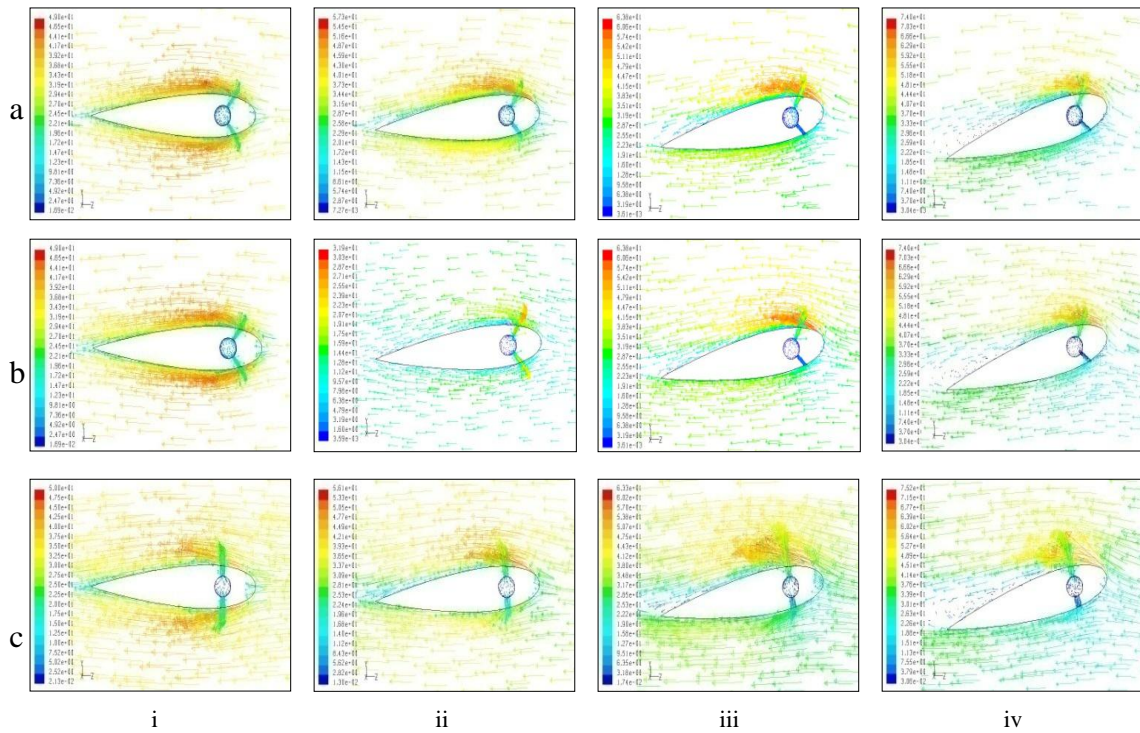
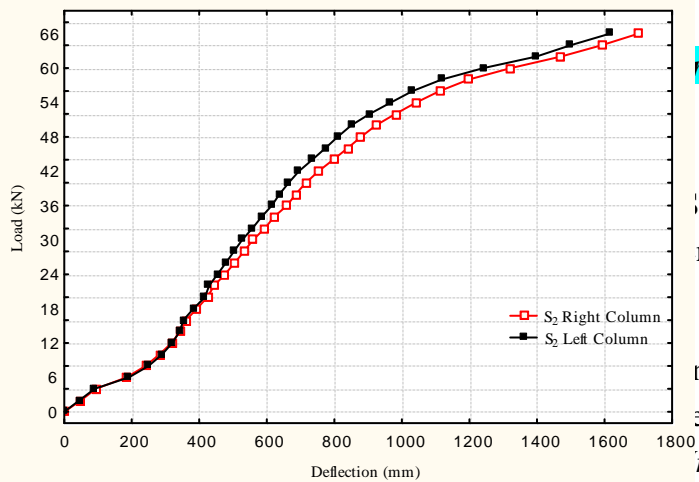


Figure (13) Velocity vectors at mid-plane of span for (a) and (b) and at $x/s=0.1$ from the injection point for (c) with $VR=1.3$ and i) $\alpha=0^\circ$, ii) $\alpha=5^\circ$, iii) $\alpha=10^\circ$ and v) $\alpha=15^\circ$.



l., Salcudean, M. and Gartshore, I. S., Multiple jets in
nts and numerical simulations, *ASME Paper 95-GT-*

nd Rodi W., Three-dimensional calculations of the
e with film cooling injection near the leading edge,
University of Karlsruhe, Kaiserstrasse 12, D-76128,

Karlsruhe, Germany, 2001.

3. Azzi, A., Abidat, M., Jubran, B. A. and Theodoridis G.S., 2001, Film cooling predictions of simple and compound angle injection from one and two staggered rows, *Numerical Heat Transfer, Part A, Vol. 40, pp. 237-294*, 2001.
4. Hussein, M. A., Experimental and computational simulation of turbine blade film cooling flow; Effect of jet angle, PHD Thesis, *University of Technology, Al-Rasheed College of Engineering and Science*, Baghdad, Iraq, June 2006.
5. Lene, K. H. and Bjorn, H. H., CFD modeling of turbulent mixing in a confined wake flow, *Aalborg University, Esbjerg*, 2003.
6. Vestige, H. K. and Malalasekera, W., An introduction to computational fluid dynamics, finite volume method, *Longman Group*, London, 1996.
7. Yang, Z. and Shih, T. H. New time scale based k- ϵ model for near – wall turbulence, *AIAA, J 31 (7), PP 1191-1197*, 1993.
8. FLUENT, 6.1, code, fluent users.com, 2002.
9. Versteeg, H.K. and Malalasekera, W., An Introduction to computational fluid dynamics the finite volume method, *Book, Longman Group*, London.1996.
10. Leylek, J. H. and Zerkle, R. D., Discrete-jet film cooling, *ASME paper 93-GT-207*, 1993.
11. Karcz, M., Performance analysis of the thermal diffusers, the gas turbine cooling aspects, *PhD Thesis*, Institute of fluid-flow machinery PAS, *Thermo-chemical power department*, Gdansk, Poland, 2003.
12. Hartsel, J. E., Prediction of effects of mass-transfer cooling on the blade row efficiency of turbine airfoil, *AIAA Paper, No. 72-11*, 1972.